Effect of image forces on polyelectrolyte adsorption at a charged surface

René Messina*
Institut für Theoretische Physik II, Heinrich-Heine-Universität Düsseldorf, Universitätsstrasse 1, D-40225 Düsseldorf, Germany
(Received 3 June 2004; published 9 November 2004)

The adsorption of flexible and highly charged polyelectrolytes onto oppositely charged planar surfaces is investigated by means of Monte Carlo simulations. The effect of image forces stemming from the dielectric discontinuity at the substrate interface is analyzed. The influence, at fixed polyelectrolyte volume fraction, of chain length and surface-charge density is also considered. A detailed structural study, including monomer and fluid charge distributions, is provided. It is demonstrated that image forces can considerably reduce the degree of polyelectrolyte adsorption and, as a major consequence, inhibit the charge inversion of the substrate by the polyelectrolytes.

DOI: 10.1103/PhysRevE.70.051802 PACS number(s): 82.35.Gh, 82.35.Rs, 61.20.Qg, 61.20.Ja

I. INTRODUCTION

The adsorption of charged polymers [polyelectrolytes (PEs)] on charged surfaces is an important phenomenon in industrial and biological processes. Well controlled model experiments [1,2] were devoted to characterize PE adsorption. The understanding of PE adsorption remains an outstanding problem because of the many different typical interactions involved there: strong electrostatic substrate-PE binding, monomer-monomer (PE-PE) repulsion, chain entropy, excluded volume, etc. Another complication arises from the *dielectric discontinuity* between the solvent and the substrate generating surface-polarization charges. In most practical cases, water plays the role of the solvent for PEs, whereas the substrate corresponds to an unpolar dielectric medium leading to considerable polarization (image) forces.

On the theoretical side, PE adsorption on planar charged surfaces has been intensively studied by several authors [3–24] on the level of mean--field theories. The case of PE adsorption on heterogeneously charged surfaces was recently theoretically addressed by de Vries *et al.* [21]. A remarkable common feature of some of these studies is the charge reversal (*overcharging*) of the substrate by the adsorbed PEs (see, e.g., Refs. [12,13,15,16,19,25]). The problem of PE adsorption onto *similarly* charged substrates was recently investigated by Dobrynin and Rubinstein [19] and Cheng and Lai [23,24]. In the latter situation, the PE adsorption is then driven either by *nonelectrostatic short-range* forces [19] or *attractive image forces* [23,24] stemming from a high-dielectric surface. The problem of *repulsive* image forces stemming from a low-dielectric surface was studied by Borisov *et al.* [9] and Netz and Joanny [16] on the level of the Debye-Hückel approximation.

As far as computer simulations are concerned, there exist few Monte Carlo (MC) studies about PE adsorption on planar charged substrates [23,26–30]. The first MC study on PE adsorption was that of Beltán *et al.* [26], where a lattice model was employed. Yamakov *et al.* [28] performed extensive MC simulations and found excellent agreement with the scaling predictions of Borisov *et al.* [9], where different regimes of adsorption are identified. Ellis *et al.* [29] considered the interesting case of heterogeneously charged surfaces (made of positively and negatively charged surface sites) and demonstrated that a PE carrying the same sign of charge as that of the net charge of the substrate can adsorb. Cheng *et al.* [23] also investigated the effect of image charges on a high-dielectric constant substrate. It is important to mention that all these MC simulations [23,26–29] use the Debye-Hückel approximation. The problem of PE multilayering was very recently studied by Messina [30], where the full unscreened long-range electrostatic interactions were considered but without image forces.

In this paper, we investigate multichain adsorption in the dilute regime at fixed PE volume fraction in a salt-free environment but where counterions from the substrate and the PEs are explicitly taken into account. In order to clearly identify the effect of image forces on PE adsorption, we systematically compare situations *with* and *without* image forces, which was not properly done in the literature (see, e.g., Refs. [9,16,24]). The influence of chain length (for short chains) and substrate-charge density is also considered. Our paper is organized as follows. The model and simulation technique are detailed in Sec. II. Our results are presented in Sec. III, and Sec. IV provides concluding remarks.

II. MODEL AND PARAMETERS

A. Simulation model

The setup of the system under consideration is similar to that recently investigated with a planar substrate (without image forces) [30]. Within the framework of the primitive model, we consider a PE solution near a charged hard wall with an implicit solvent (water at $z>0$) of relative dielectric permittivity $\epsilon_{\mathrm{solv}}\approx 80$. The substrate located at $z<0$ is characterized by a relative dielectric permittivity ϵ_{subs} which leads to a dielectric jump Δ_ϵ (when $\epsilon_{\mathrm{solv}}\neq\epsilon_{\mathrm{subs}}$) at the interface defined as

$$\Delta_\epsilon = \frac{\epsilon_{\mathrm{solv}} - \epsilon_{\mathrm{subs}}}{\epsilon_{\mathrm{solv}} + \epsilon_{\mathrm{subs}}} \geqslant 0. \qquad (1)$$

*Electronic address: messina@thphy.uni-duesseldorf.de

The *negative* bare surface-charge density of the substrate is $-\sigma_0 e$, where e is the (positive) elementary charge and $\sigma_0 > 0$ is the number of charges per unit area. Electroneutrality is always ensured by the presence of explicit monovalent ($Z_c = 1$) substrate counterions (i.e., monovalent cations) of diameter a. PE chains are made up of N_m *monovalent* positively charged monomers ($Z_m = 1$) of diameter a. Each monomer is charged so that the fraction of charged monomers is unity. Their counterions (monovalent anions) are also explicitly taken into account with the same parameters up to the charge sign as the monomers. Hence, all microions are monovalent: $Z = Z_c = Z_m = 1$ with the same diameter size a.

All these particles making up the system are immersed in a rectangular $L \times L \times \tau$ box. Periodic boundary conditions are applied in the (x,y) directions, whereas hard walls are present at $z = 0$ (location of the charged interface) and $z = \tau$ (location of an *uncharged* wall).

The total energy of interaction of the system can be written as

$$U_{\text{tot}} = \sum_i [U_{\text{hs}}^{(\text{plate})}(z_i) + U_{\text{Coul}}^{(\text{plate})}(z_i)] + \sum_{i,i<j} [U_{\text{hs}}(r_{ij}) + U_{\text{Coul}}(\mathbf{r}_i, \mathbf{r}_j) + U_{\text{FENE}}(r_{ij}) + U_{\text{LJ}}(r_{ij})], \quad (2)$$

where the first (single) sum stems from the interaction between an ion i (located at $z = z_i$) and the charged plate, and the second (double) sum stems from the pair interaction between ions i and j with $r_{ij} = |\mathbf{r}_i - \mathbf{r}_j|$. All these contributions to U_{tot} in Eq. (2) are described in detail below.

Excluded volume interactions are modeled via a hardcore potential [31] defined as follows:

$$U_{\text{hs}}(r_{ij}) = \begin{cases} 0 & \text{for } r_{ij} \geqslant a \\ \infty & \text{for } r_{ij} < a \end{cases} \quad (3)$$

for the microion-microion one, and

$$U_{\text{hs}}^{(\text{plate})}(z_i) = \begin{cases} 0 & \text{for } a/2 \leqslant z_i \leqslant \tau - a/2 \\ \infty & \text{otherwise} \end{cases} \quad (4)$$

for the plate-microion one. For clarity, we recall that a microion stands either for a (charged) monomer or a counterion.

The electrostatic energy of interaction between two microions i and j reads

$$\beta U_{\text{Coul}}(\mathbf{r}_i, \mathbf{r}_j) = \pm l_B \left[\frac{1}{r_{ij}} + \frac{\Delta_\epsilon}{\sqrt{x_{ij}^2 + y_{ij}^2 + (z_i + z_j)^2}} \right], \quad (5)$$

where $+$ $(-)$ applies to microions of the same (opposite) sign, $l_B = \beta e^2 / 4\pi\epsilon_0\epsilon_{\text{solv}}$ is the Bjerrum length corresponding to the distance at which two protonic charges interact with $1/\beta = k_B T$, and Δ_ϵ is given by Eq. (1). The first term in Eq. (5) corresponds to the direct Coulomb interaction between real ions, whereas the second term represents the interaction between the real ion i and the image of ion j. By symmetry, the latter also describes the interaction between the real ion j and the image of ion i yielding an implicit factor $1/2$. The electrostatic energy of interaction between an ion i and the (uniformly) charged plate reads

TABLE I. List of key parameters with some fixed values.

Parameters	
$T = 298$ K	room temperature
$\sigma_0 L^2$	charge number of the substrate
$\Delta_\epsilon = 0$ or 0.951	dielectric discontinuity
$Z = 1$	microion valence
$a = 4.25$ Å	microion diameter
$l_B = 1.68a = 7.14$ Å	Bjerrum length
$L = 25a$	(x,y)-box length
$\tau = 75a$	z-box length
N_{PE}	number of PEs
N_m	number of monomers per chain

$$\beta U_{\text{Coul}}^{(\text{plate})}(z_i) = l_B \left[\pm 2\pi\sigma_0 z_i + \frac{\Delta_\epsilon}{4z_i} \right], \quad (6)$$

where, for the first term, $+$ $(-)$ applies to positively (negatively) charged ions. The second term in Eq. (6) stands for the *self-image* interaction, i.e., the interaction between the ion i and its own image. An appropriate and efficient modified Lekner sum was utilized to compute the electrostatic interactions with periodicity in *two* directions [32]. To link our simulation parameters to experimental units and room temperature ($T = 298$ K), we choose $a = 4.25$ Å leading to the Bjerrum length of water $l_B = 1.68a = 7.14$ Å. In order to investigate the effect of image forces, we take a value of $\epsilon_{\text{subs}} = 2$ for the dielectric constant of the charged substrate (which is a typical value for silica or mica substrates [33]) and $\epsilon_{\text{solv}} = 80$ for that of the aqueous solvent yielding $\Delta_\varepsilon = (80-2)/(80+2) \approx 0.951$. The case of identical dielectric constants $\epsilon_{\text{solv}} = \epsilon_{\text{subs}}$ $(\Delta_\epsilon = 0)$ corresponds to the situation where there are no image charges.

The PE chain connectivity is modeled by employing a standard finite extension nonlinear elastic (FENE) potential for good solvent, which reads

$$U_{\text{FENE}}(r) = \begin{cases} -\frac{1}{2}\kappa R_0^2 \ln\left[1 - \frac{r^2}{R_0^2}\right] & \text{for } r < R_0 \\ \infty & \text{for } r \geqslant R_0 \end{cases} \quad (7)$$

with $\kappa = 27 k_B T / a^2$ and $R_0 = 1.5a$. The excluded volume interaction between chain monomers is taken into account via a shifted and truncated Lennard-Jones (LJ) potential given by

$$U_{\text{LJ}}(r) = \begin{cases} 4\epsilon\left[\left(\frac{a}{r}\right)^{12} - \left(\frac{a}{r}\right)^{6}\right] + \epsilon & \text{for } r \leqslant 2^{1/6}a \\ 0 & \text{for } r > 2^{1/6}a \end{cases}, \quad (8)$$

where $\epsilon = k_B T$. These parameter values lead to an equilibrium bond length $l = 0.98a$.

All the simulation parameters are gathered in Table I. The set of simulated systems can be found in Table II. The equilibrium properties of our model system were obtained by using standard canonical MC simulations following the Metropolis scheme [34,35]. Single-particle moves were considered with an acceptance ratio of 30% for the monomers and

TABLE II. Simulated systems' parameters. The number of counterions (cations and anions) ensuring the overall electroneutrality of the system is not indicated.

System	N_{PE}	N_m	$\sigma_0 L^2$
A	96	2	64
B	48	4	64
C	24	8	64
D	12	16	64
E	6	32	64
F	12	16	32
G	12	16	128
H	12	16	192

50% for the counterions. Depending on the parameters, the length of a simulation run ranges from 2×10^6 up to 7×10^6 MC steps per particle. Typically, about 3×10^5 to 2.5×10^6 MC steps were required for equilibration, and $(1-4)\times10^6$ subsequent MC steps were used to perform measurements.

B. Measured quantities

We briefly describe the different observables that are going to be measured. In order to study the PE adsorption, we compute the monomer density $n(z)$ that is normalized as follows:

$$\int_{a/2}^{\tau-a/2} n(z)L^2dz = N_{\mathrm{PE}}N_m. \tag{9}$$

To further characterize the PE adsorption, we also compute the total number of accumulated monomers $\overline{N}(z)$ within a distance z from the planar charged plate that is given by

$$\overline{N}(z) = \int_{a/2}^{z} n(z')L^2dz'. \tag{10}$$

It is useful to introduce the fraction of adsorbed monomers, $N^*(z)$, which is defined as follows:

$$N^*(z) = \frac{\overline{N}(z)}{N_{\mathrm{PE}}N_m}. \tag{11}$$

Another relevant quantity is the global *net fluid charge* $\sigma(z)$, which is defined as follows:

$$\sigma(z) = \int_{a/2}^{z} [n_+(z') - n_-(z')]dz', \tag{12}$$

where n_+ and n_- stand for the density of all the positive microions (i.e., monomers and plate's counterions) and negative microions (i.e., PEs' counterions), respectively. It is useful to introduce the reduced surface charge density $\sigma^*(z)$ defined as follows:

$$\sigma^*(z) = \frac{\sigma(z)}{\sigma_0}. \tag{13}$$

Thereby, $\sigma^*(z)$ corresponds, up to a prefactor $\sigma_0 e$, to the net fluid charge per unit area (omitting the surface charge density $-\sigma_0 e$ of the substrate) within a distance z from the charged wall. At the uncharged wall, electroneutrality imposes $\sigma^*(z=\tau-a/2)=1$. By simple application of Gauss' law, $[\sigma^*(z)-1]$ is directly proportional to the mean electric field at z. Therefore, $\sigma^*(z)$ can measure the *screening* strength of the substrate by the neighboring solute charged species.

III. RESULTS AND DISCUSSION

From previous studies [9,16,36,37], it is well understood that effects of image charges become especially relevant at sufficiently low surface charge density of the interface. It is also clear that the self-image interaction (*repulsive* for $\Delta_\epsilon>0$, as is presently the case) is higher the higher the charge of the ions (polyions) since it scales like Z^2. In the present situation where we have to deal with PEs, the length of the chain (N_m) is a key parameter that can be seen as the valence of a polyion. Hence, we are going to study (i) the influence of chain length (Sec. III A) and (ii) that of surface charge density (Sec. III B). For the sake of consistency, we fixed the total number of monomers to $N_{\mathrm{PE}}N_m=192$, meaning that the monomer concentration is *fixed* (see also Table II): The PE volume fraction

$$\phi = \frac{4\pi}{3}\frac{N_{\mathrm{PE}}N_m(a/2)^3}{L^2\tau} \approx 2.14\times10^{-3}$$

is fixed.

A. Influence of chain length

In this part, we consider the influence of chain length N_m at fixed surface charge density parameter $\sigma_0L^2=64$. The latter corresponds experimentally to a moderate [2] surface charge density with $-\sigma_0 e\approx-0.091$ C/m^2. The chain length is varied from $N_m=2$ up to $N_m=32$ (systems $A-E$, see Table II). We have ensured that, for the longest chain with $N_m=32$, size effects are still negligible since the mean end-to-end distance is about $14a$, which is significantly smaller than $L=25a$ or $\tau=75a$.

The profiles of the monomer distribution $n(z)$ can be found in Fig. 1 and the corresponding microstructures are sketched in Fig. 2. Let us first comment on the more simple case where no image charges are present [$\Delta_\epsilon=0$—see Fig. 1(a)]. For (very) short chains (here $N_m\leqslant4$), Fig. 1(a) shows that the density profiles exhibit a monotonic behavior even near contact. Within this regime of chain length, the monomer density near the charged wall increases with increasing N_m. This feature is fully consistent with the idea that stronger *lateral* correlations, the latter scaling like $Z^{3/2}$ for spherical counterions at fixed σ_0 [38,39], induce a higher polyion adsorption. In other words, at (very) low N_m, *conformational entropic* effects are not dominant and the short-chains systems can be qualitatively understood with the picture provided by spherical (or pointlike) ions. The scenario becomes

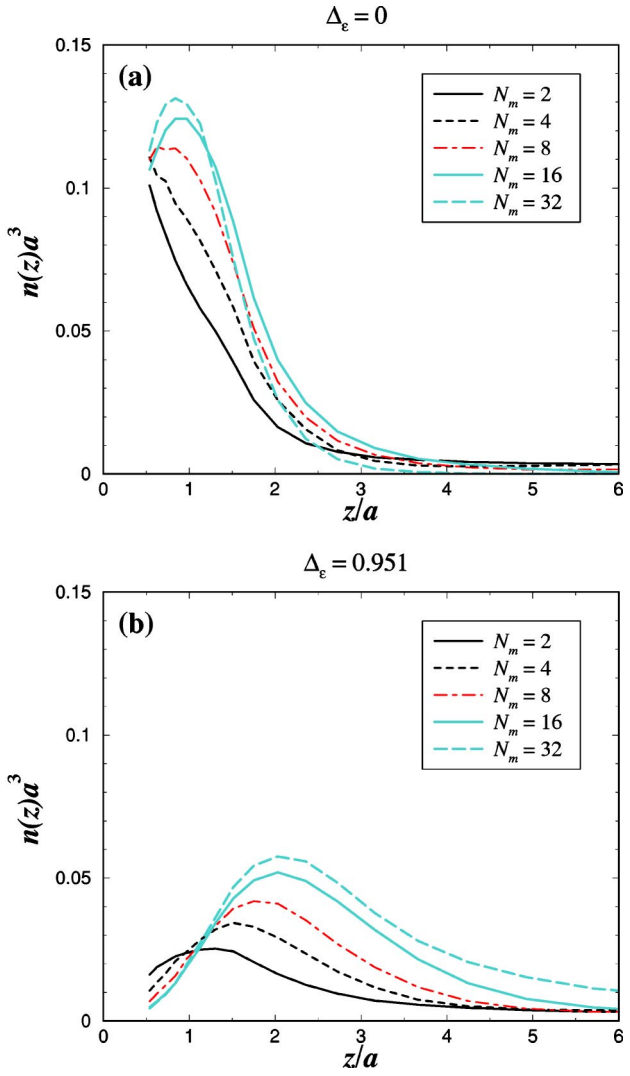

FIG. 1. Profiles of the monomer density $n(z)$ for different chain length N_m with $\sigma_0 L^2=64$ (systems $A-E$). (a) $\Delta_\epsilon=0$. (b) $\Delta_\epsilon=0.951$.

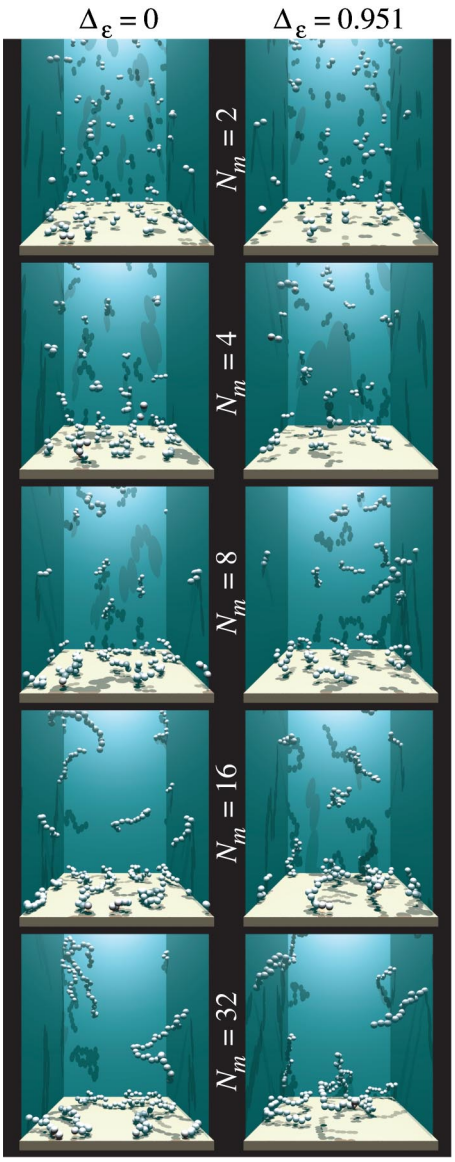

FIG. 2. Typical equilibrium microstructures of systems $A-E$. The little counterions are omitted for clarity.

qualitatively different at higher chain length [here $N_m \geqslant 8$—see Fig. 1(a)], where $n(z)$ presents a maximum near contact which is the signature of a *short-range repulsion* that was also theoretically predicted [10]. This nontrivial feature can be explained in terms of entropy: Near the surface of the substrate, the number of available PE conformations is considerably reduced, yielding to an entropic repulsion that can be detected if the driving force of PE adsorption (crucially controlled by σ_0) is not strong enough. This latter statement will be properly examined and confirmed in Sec. III B, where the influence of σ_0 is addressed. Nonetheless, the highest value of $n(z;N_m)$ increases with N_m, as it should be. All these mentioned features can be visualized on the microstructures depicted in Fig. 2. One can summarize those relevant findings, valid for small enough σ_0 and $\Delta_\epsilon=0$, as follows: (i) For very short chains, the PE adsorption is similar to that occurring with spherical electrolytes; (ii) PE chains experience a short-range repulsion near the substrate due to conformational entropic effects. Now, at *true* contact (i.e., $z=0.5a$) it seems that the monomer density $n(z \rightarrow a/2)$ [40] seems to be nearly independent of N_m for the parameters under consideration. In fact, for a (one-component) electrolyte, the density at contact can be *exactly* obtained [41] via the relation $n(z=a/2)-n(z=\tau-a/2)=2\pi l_B \sigma_0^2$ yielding $n(z=a/2)\approx 0.11a^{-3}$ [where basically $n(z=\tau-a/2)\approx 0$], which is in remarkable agreement with the value found in Fig. 1(a). One can wonder why such a simple theorem is "equally" well satisfied for PE systems that significantly deviate from simple structureless spherical ions. In fact, this is a nontrivial finding since already for *rodlike* PEs a fully different behavior is observed. Certainly more data are needed to clarify this point.

We now turn to the more complicated situation where image forces are present [$\Delta_\epsilon=0.951$—see Fig. 1(b)]. An immediate remark that can be drawn from a comparison with the $\Delta_\epsilon=0$ case is that the PE adsorption is much weaker due to the repulsive image-polyion interactions. At all N_m, $n(z)$ presents a maximum at $z=z^*$ that is gradually shifted to larger z with increasing N_m. In other words, the *thickness* of

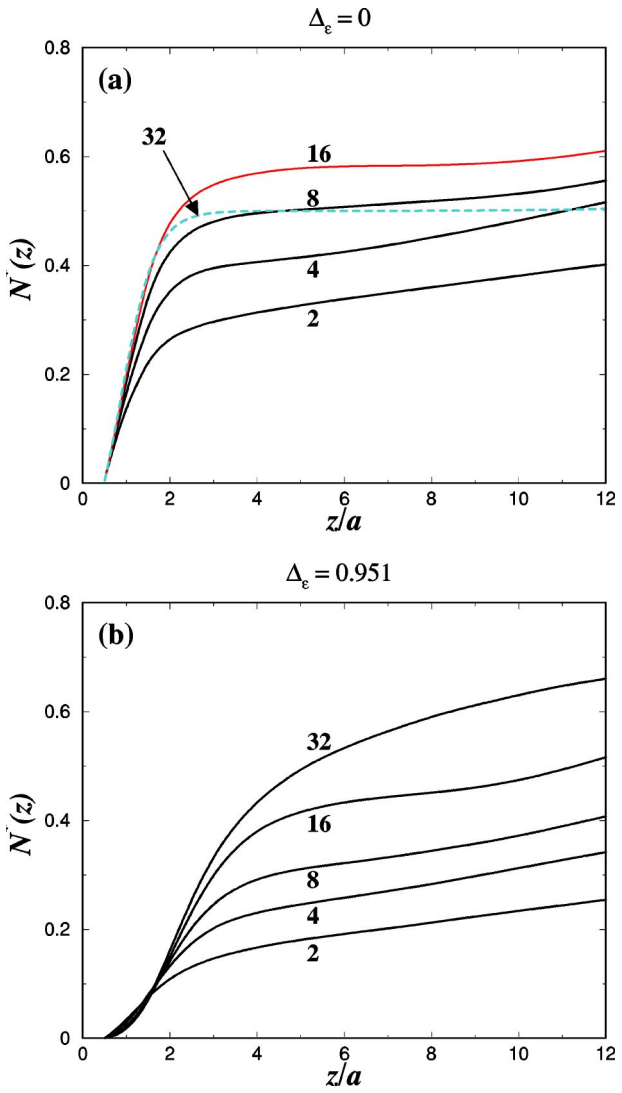

FIG. 3. Profiles of the fraction of adsorbed monomers $N^*(z)$ for different chain length N_m (as indicated by its numerical value) with $\sigma_0 L^2=64$ (systems $A-E$). (a) $\Delta_\epsilon=0$. (b) $\Delta_\epsilon=0.951$.

the adsorbed PE layer as determined by z^* increases with N_m. This phenomenon is of course due to the fact that the image-polyion repulsion increases with N_m, similarly to what happens with multivalent (pointlike or spherical) counterions [36,37]. On the other hand, interestingly, the monomer density at contact *decreases* with increasing N_m. This is the result of a *combined* effect of (i) conformational entropy as explained above and (ii) the N_m-induced image-polyion repulsion. All those features are well illustrated on the microstructures of Fig. 2.

To gain further insight into the properties of PE adsorption, we have plotted the fraction of adsorbed monomers $N^*(z)$ [Eq. (11)] in Fig. 3. At $\Delta_\epsilon=0$ [see Fig. 3(a)], it is observed in the immediate vicinity of the wall (roughly for $z \lesssim 1.5a$) that $N^*(z;N_m)$ increases monotonically with N_m, as expected. However, further away from the wall, a nontrivial effect is found where $N^*(z;N_m)$ surprisingly exhibits a nonmonotonic behavior with respect to N_m. More explicitly, in the regime of large N_m we have $N^*(z;N_m=32)$, which is clearly smaller than $N^*(z;N_m=16)$ and even smaller than $N^*(z;N_m=8)$ when one is sufficiently far from the wall. This remarkable phenomenon is going to be explained later by advocating the role of overcharging. Upon switching the image forces on [$\Delta_\epsilon=0.951$—see Fig. 3(b)], $N^*(z;N_m)$ shows a qualitatively different behavior from that found at $\Delta_\epsilon=0$, in accordance with our study concerning $n(z)$. More precisely, (i) very close to the wall, $N^*(z;N_m)$ *decreases* with N_m, while (ii) sufficiently far away from the wall, $N^*(z;N_m)$ *increases* with N_m. This behavior is fully consistent with our mechanisms previously discussed for $n(z)$. Below, we are going to show that the reduced net fluid charge $\sigma^*(z)$ is a key observable to account for those reported properties of $N^*(z;N_m)$.

A deeper understanding of the physical mechanisms involved in PE adsorption can be gained by considering the net fluid charge parameter $\sigma^*(z)$ [Eq. (13)] that describes the screening of the charged interface. The profiles of $\sigma^*(z)$ for different N_m can be found in Fig. 4. At $\Delta_\epsilon=0$ [see Fig. 4(a)], it is shown that for long enough chains (here $N_m \geqslant 4$) the substrate gets locally *overcharged*, as signaled by $\sigma^*(z)>1$. Physically, this means that the global local charge of the adsorbed monomers [42] is larger in absolute value than that of the interface. In other words, the charged wall is *overscreened* by the adsorbed PE chains. Figure 4(a) indicates that the degree of overcharging increases with N_m, as expected from the behavior of multivalent counterions, and seems to saturate at high N_m. This enhanced N_m overcharging leads to a sufficiently strong effective repulsion between the substrate and the PEs in the solution, which in turn prevents further adsorption. It is precisely this mechanism that explains the apparent anomaly found in Fig. 3(a), where, sufficiently away from the surface, it was reported a significantly lower monomer fraction $N^*(z;N_m)$ at $N_m=32$ than at $N_m=16$ or $N_m=8$. That is to say, although the amount of overcharging is essentially the same for $N_m=32$ and $N_m=16$, the *effective repulsive* interaction between the wall (covered by the adsorbed PEs) and the nonadsorbed PEs increases with N_m, leading to a stronger PE depletion above the PE layer at large enough N_m. This spectacular effect (due to electrostatic correlations) is well illustrated in Fig. 2 (with $N_m=32$), where above the (strongly bound) adsorbed PEs there is a depletion zone.

Upon inducing polarization charges [$\Delta_\epsilon=0.951$—see Fig. 4(b)], overscreening is canceled. This, in turn, accounts for the absence of plateau in $N^*(z;N_m)$ at $\Delta_\epsilon=0.951$. That striking disappearance of overcharging can be rationalized by establishing again an analogy with multivalent spherical ions, as follows.

For the sake of simplicity, let us assume that the PE can be electrostatically envisioned as a spherical polyion of valence N_m with a radius corresponding roughly to the radius of gyration of the chain. Thereby, the image-polyion *repulsive* interactions [including the self-image repulsion as well as the lateral image-ion correlations as given by the second term of Eq. (5)] scale like N_m^2, whereas the *attractive* driving force of polyion adsorption due to Wigner crystal ordering scales like $N_m^{3/2}$ [37]. The latter driving force corresponds to the highest possible attraction between the substrate and the polyion, and

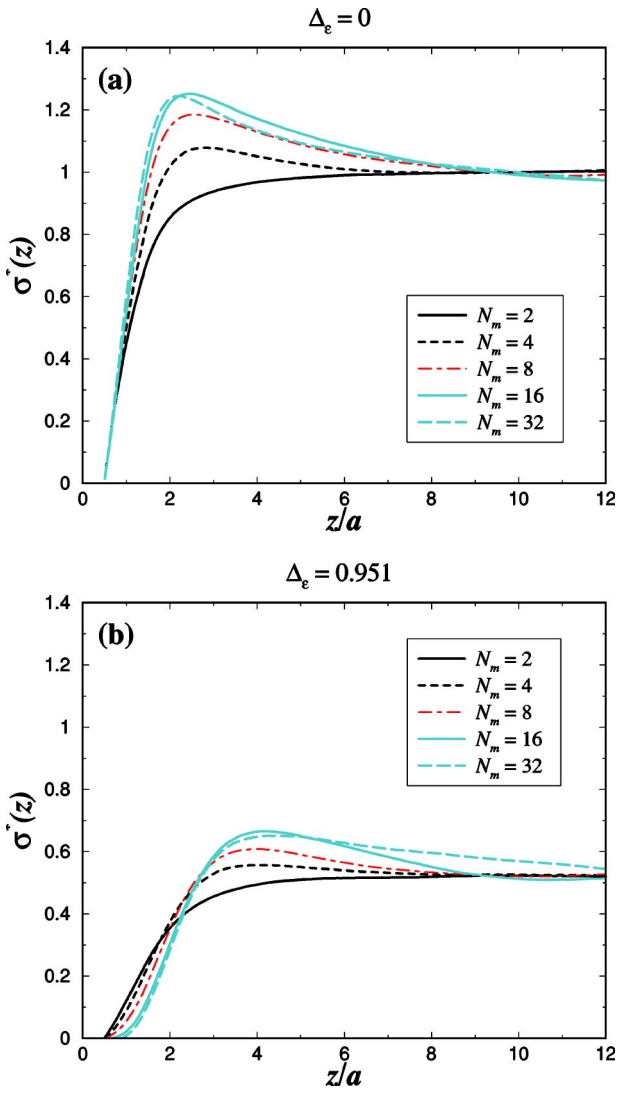

FIG. 4. Profiles of the reduced net fluid charge $\sigma^*(z)$ for different chain length N_m with $\sigma_0 L^2=64$ (systems $A-E$). (a) $\Delta_\epsilon=0$. (b) $\Delta_\epsilon=0.951$.

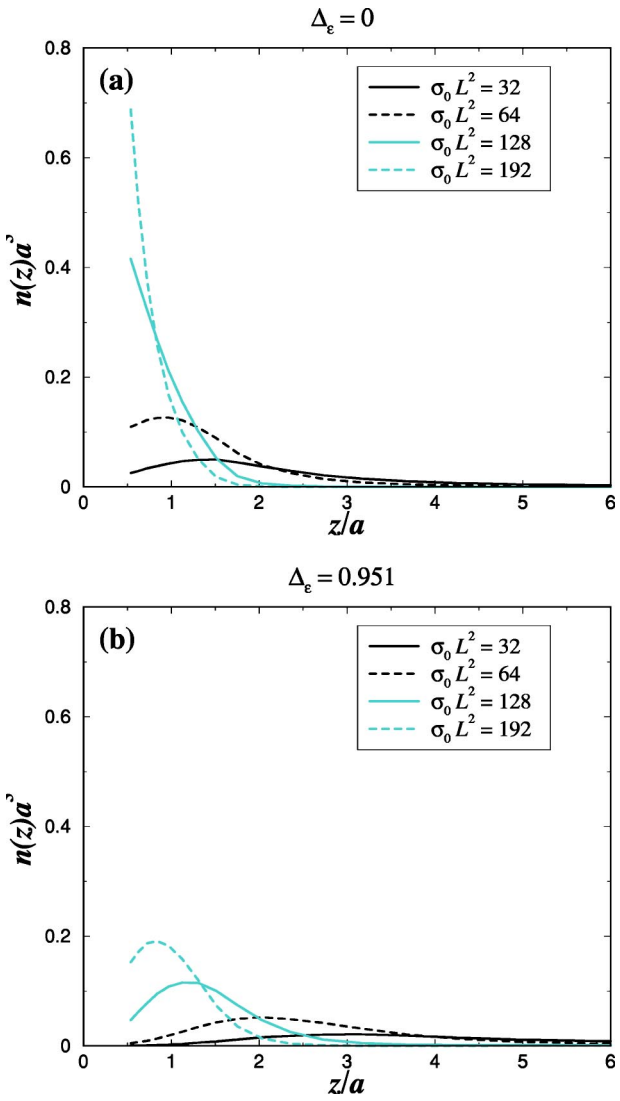

FIG. 5. Profiles of the monomer density $n(z)$ for different parameters of surface charge density $\sigma_0 L^2$ with $N_m=16$ (systems $D,F-H$). The case $\sigma_0 L^2=64$ (system D) from Fig. 1 is reported here again for easier comparison. (a) $\Delta_\epsilon=0$. (b) $\Delta_\epsilon=0.951$.

is therefore a good candidate for the present discussion. Consequently, at large enough N_m, image forces are dominant and inhibit overcharging.

This behavior strongly contrasts with the case of *spherical* substrates, where image forces do not affect the occurrence of overcharging [37].

B. Influence of substrate surface-charge density

To complete our investigation, we would like to address the influence of the substrate charge density on the PE adsorption in the presence of image forces. In this respect, we consider (at fixed $N_m=16$) three additional values of the charge density: $\sigma_0 L^2=32$, 128, 192 corresponding to the systems F,G,H, respectively (see Table II).

The plots of the monomer density $n(z)$ at various values of $\sigma_0 L^2$ can be found in Fig. 5. Microstructures of systems F and H are presented in Fig. 6. At $\Delta_\epsilon=0$ [see Fig. 5(a)], the monomer density at contact increases with σ_0 as it should be. Interestingly, the local maximum in $n(z)$ [present at small σ_0 (here $\sigma_0 L^2 \leqslant 64$)] *vanishes at large* σ_0 [see Fig. 5(a)]. This feature is the result of a σ_0-enhanced driving force of adsorption that overcomes entropic effects at large enough σ_0. The strong adsorption at $\sigma_0 L^2=192$ leads to a *flat* PE layer as well, illustrated in Fig. 6.

By polarizing the substrate surface ($\Delta_\epsilon=0.951$), it can be seen from Fig. 5(b) and the snapshot of Fig. 6 that there is a strong monomer depletion near contact at $\sigma_0 L^2=32$. This feature is due to the combined effects of (i) conformational entropy, (ii) image-monomer repulsion, and (iii) a lower electrostatic wall-monomer attraction. Upon increasing σ_0, the monomer density near contact becomes larger, and concomitantly, the maximum in $n(z)$ is systematically shifted to smaller z. That is to say, the thickness of the adsorbed PE layer decreases with σ_0.

The profiles of $N^*(z)$ are provided in Fig. 7, from which further characterization of PE adsorption can be obtained. At

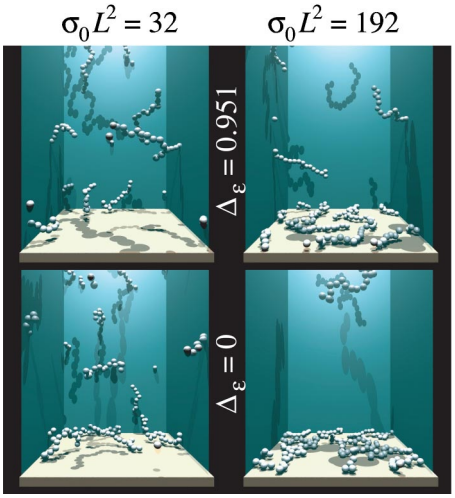

FIG. 6. Typical equilibrium microstructures of systems *F* and *H*. The little counterions are omitted for clarity.

$\Delta_\epsilon=0$, Fig. 7(a) indicates that $N^*(z;\sigma_0)$ increases with σ_0 but saturates at high σ_0. This latter saturation effect should only be relevant for a regime of charge where $\eta \equiv N_{\mathrm{PE}}N_m/\sigma_0 L^2$ is about unity. Indeed, in a typical experimental situation at finite monomer concentration (even in the dilute regime), we have $\eta \gg > 1$ so that overcharging is always possible at large σ_0 and thereby $N^*(z;\sigma_0)$ should always significantly increase with σ_0 as long as packing effects (as generated by the excluded volume of the monomers) are not vivid. In parallel, the plateau reported at $\sigma_0 L^2=128$ and $\sigma_0 L^2=192$ in Fig. 7(a) is the signature of a monomer depletion above the adsorbed PE layer (see also Fig. 6) due to a strong screening of the surface charge by the latter. At $\Delta_\epsilon=0.951$, Fig. 7(b) shows that $N^*(z)$ is considerably smaller than at $\Delta_\epsilon=0$ even for high σ_0, in accordance with the behavior of $n(z)$ from Fig. 5. The Δ_ϵ-induced desorption is especially strong at $\sigma_0 L^2=32$, where the image-monomer repulsion clearly counterbalances the electrostatic wall-monomer attraction. More quantitatively, at $z=3a$ (a z distance corresponding roughly to the radius of gyration of the chain with $N_m=16$), about 30% [i.e., $N^*(z)=0.3$] of the monomers are adsorbed with $\Delta_\epsilon=0$ against only 10% with $\Delta_\epsilon=0.951$ [see Fig. 7(b)].

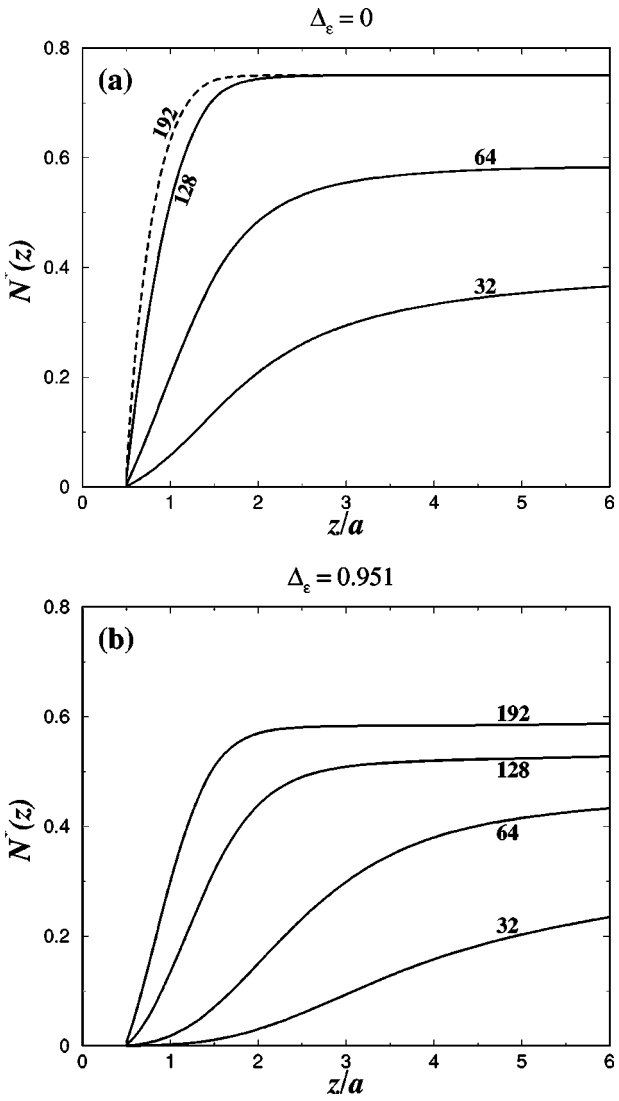

FIG. 7. Profiles of the fraction of adsorbed monomers $N^*(z)$ for different parameters of surface charge density $\sigma_0 L^2$ (as indicated by its numerical value) with $N_m=16$ (systems *D*,*F*-*H*). The case $\sigma_0 L^2=64$ (system *D*) from Fig. 3 is reported here again for easier comparison. (a) $\Delta_\epsilon=0$. (b) $\Delta_\epsilon=0.951$.

IV. CONCLUDING REMARKS

We first would like to make some final remarks about the presented results. As far as the charge surface distribution on the substrate's surface is concerned, we have assumed a *smeared-out* one in contrast to a real experimental situation where it is *discrete*. Previous numerical studies [43–45] have shown that the counterion distribution at inhomogeneously charged substrates may deviate from that obtained at smeared-out ones at strong Coulomb coupling (i.e., multivalent counterions and/or high Bjerrum length) or strong substrate charge modulations. Nonetheless, at standard Bjerrum length (i.e., $l_B=7.1$ Å for water at room temperature, as is presently the case) and with discrete monovalent ions generating the substrate's surface charge, it has been demonstrated that the counterion distribution is marginally modified [43] even for trivalent counterions. Hence, we think that our results will not qualitatively differ from the more realistic situation of non-smeared-out substrate charges consisting of discrete monovalent ions.

Another approximation in our model is the location of the dielectric discontinuity. More precisely, it was implicitly assumed that the latter coincides with the charged interface (considered here as a hard wall). In fact, experimentally, it is not clear where the dielectric discontinuity is located and the transition is rather gradual and spreads out over several angstroms [46], so that in a continuum description the dielectric discontinuity might be located somewhat below the *hard* interface. In this respect, our model tends to slightly overestimate the effect of image forces and namely, with $\Delta_\epsilon>0$, the self-image *repulsion*. Furthermore, in the presence of *short-range* attractive interactions between the substrate and the

PEs (for instance, stemming from some specific chemical properties of the chains and the substrate, i.e., chemisorption), the effect of image charges might also be reduced [19]. This means that the substrate-charge *undercompensation* by PEs induced by repulsive image forces as reported in Fig. 4(b) is dependent on the relative strength of that short-range attractive interaction, which is not taken into account in our model. Nevertheless, we are confident that our results provide a reliable fingerprint for the understanding of the effect of image forces on PE adsorption in a salt-free environment.

It is not a straightforward task to access experimentally these effects stemming from image forces. One major difficulty arises from the fact that by changing the dielectric constant of the solvent, ϵ_{solv}, one changes the degree of ionization of the PEs. However, there is the experimental possibility to tune Δ_ϵ by using *organic* solvents (i.e., with a low ϵ_{solv} but still polar) with a mixture of large colloidal particles [e.g., latex particles with weak curvature and (low) dielectric constant ϵ_{subs} such that $\epsilon_{\mathrm{subs}} \leqslant \epsilon_{\mathrm{solv}}$] and PEs. In this experimental context, one should be able to verify the trends of our current findings.

To conclude, we have performed MC simulations to address the effect of image forces on PE adsorption at oppositely charged planar substrates. The influence of chain length and surface-charge density was also considered. We have considered a finite monomer concentration in the dilute regime for relatively short chains. Our main findings can be summarized as follows.

(i) For very short chains (here $N_m \leqslant 4$) and with no image forces (i.e., $\Delta_\epsilon = 0$), the PE adsorption is similar to that occurring with little (spherical) multivalent counterions. For longer chains (here $N_m \geqslant 8$), the PEs experience (even at $\Delta_\epsilon = 0$) a short-range repulsion near the substrate due to chain entropy effects. This latter feature is especially relevant at low substrate charge σ_0.

(ii) At fixed σ_0 and in the presence of repulsive *image forces* (here $\Delta_\epsilon = 0.951$), it was demonstrated that the monomer depletion in the vicinity of the substrate as well as the thickness of the PE layer grow with chain length N_m. Concomitantly, and as a major result, the *charge reversal* of the substrate by the adsorbed PEs *vanishes*. This latter point was in fact overlooked in the literature (see, e.g., Refs. [9,15,16,24]).

(iii) Upon varying σ_0 at fixed N_m, it was shown at $\Delta_\epsilon = 0$ that the net substrate-PE force becomes purely attractive at sufficiently high σ_0, where chain-entropy effects are overcompensated. When image forces are present, the PE *depletion* near the substrate as well as the thickness of the adsorbed PE layer decrease with σ_0.

A future work will address the adsorption of stiff *rodlike* PEs. This situation was recently theoretically examined by Cheng and de la Cruz [22]. Nonetheless, simulation data would be of great help to further characterize the arrangement of the rodlike charged particles near the interface as well as to elucidate the influence of image forces on the latter.

ACKNOWLEDGMENTS

The author thanks H. Löwen for enlightening discussions. The SFB TR6 is acknowledged for financial support.

[1] N. Hansupalak and M. M. Santore, Langmuir **19**, 7423 (2003).
[2] A. Tulpar and W. A. Ducker, J. Phys. Chem. B **108**, 1667 (2004).
[3] F. W. Wiegel, J. Phys. A **10**, 299 (1977).
[4] H. A. Van der Schee and J. Lyklema, J. Phys. Chem. **88**, 6621 (1984).
[5] M. Muthukumar, J. Chem. Phys. **86**, 7230 (1987).
[6] M. R. Böhmer, O. A. Evers, and J. M. H. M. Scheutjens, Macromolecules **23**, 2288 (1990).
[7] R. Varoqui, A. Johner, and A. Elaissari, J. Chem. Phys. **94**, 6873 (1991).
[8] R. Varoqui, J. Phys. II **3**, 1097 (1993).
[9] O. V. Borisov, E. B. Zhulina, and T. M. Birshtein, J. Phys. II **4**, 913 (1994).
[10] I. Borukhov, D. Andelman, and H. Orland, Europhys. Lett. **32**, 499 (1995).
[11] X. Châtellier and J.-F. Joanny, J. Phys. II **6**, 1669 (1996).
[12] P. Linse, Macromolecules **29**, 326 (1996).
[13] V. Shubin and P. Linse, Macromolecules **30**, 5944 (1997).
[14] I. Borukhov, D. Andelman, and H. Orland, Macromolecules **31**, 1665 (1998).
[15] J. F. Joanny, Eur. Phys. J. B **9**, 117 (1999).
[16] R. R. Netz and J. F. Joanny, Macromolecules **32**, 9013 (1999).
[17] A. V. Dobrynin, A. Deshkovski, and M. Rubinstein, Phys. Rev. Lett. **84**, 3101 (2000).
[18] A. V. Dobrynin, A. Deshkovski, and M. Rubinstein, Macromolecules **34**, 3421 (2001).
[19] A. V. Dobrynin and M. Rubinstein, J. Phys. Chem. B **107**, 8260 (2003).
[20] A. Shafir, D. Andelman, and R. R. Netz, J. Chem. Phys. **119**, 2355 (2003).
[21] R. de Vries, F. Weinbreck, and C. G. de Kruif, J. Chem. Phys. **118**, 4649 (2003).
[22] H. Cheng and O. de la Cruz, J. Chem. Phys. **119**, 12 635 (2003).
[23] C.-H. Cheng and P.-Y. Lai, e-print cond-mat/0312315.
[24] C.-H. Cheng, and P.-Y. Lai, e-print cond-mat/0403722.
[25] A. Y. Grosberg, T. T. Nguyen, and B. I. Shklovskii, Rev. Mod. Phys. **74**, 329 (2002).
[26] S. Beltrán, H. H. Hooper, H. W. Blanch, and J. M. Prausnitz, Macromolecules **24**, 3178 (1991).
[27] C. Y. Kong and M. Muthukumar, J. Chem. Phys. **109**, 1522 (1998).
[28] V. Yamakov, A. Milchev, O. Borisov, and B. Dunweg, J. Phys.: Condens. Matter **11**, 9907 (1999).
[29] M. Ellis, C. Y. Kong, and M. Muthukumar, J. Chem. Phys. **112**, 8723 (2000).
[30] R. Messina, Macromolecules **37**, 621 (2004).
[31] Only the monomer-monomer excluded volume interaction was

not modeled by a hard-sphere potential. There, a purely repulsive Lennard-Jones potential was used.
[32] A. Grzybowsky and A. Brodka, Mol. Phys. **100**, 1017 (2002).
[33] M. D. Malinsky, K. L. Kelly, G. C. Schatz, and R. P. van Duyne, J. Phys. Chem. B **105**, 2343 (2001).
[34] N. Metropolis *et al.*, J. Chem. Phys. **21**, 1087 (1953).
[35] M. P. Allen and D. J. Tildesley, *Computer Simulations of Liquids* (Clarendon Press, Oxford, 1987).
[36] G. M. Torrie, J. P. Valleau, and G. N. Patey, J. Chem. Phys. **76**, 4615 (1982).
[37] R. Messina, J. Chem. Phys. **117**, 11062 (2002).
[38] B. Shklovskii, Phys. Rev. E **60**, 5802 (1999).
[39] R. Messina, C. Holm, and K. Kremer, Phys. Rev. E **64**, 021405 (2001).
[40] Note that in a simulation, the density at contact $n(z \to a/2)$ can only be obtained by extrapolation.
[41] See, for instance, H. Wennerström, B. Jönsson, and P. Linse, J. Chem. Phys. **76**, 4665 (1982).
[42] Near the wall, the presence of the counterions at $\Delta_\epsilon = 0$ is marginal so that the fluid charge is quasiexclusively provided by the charges of the adsorbed monomers. This becomes especially vivid when $N_m \geqslant 4$, where overcharging occurs.
[43] R. Messina, Physica A **308**, 59 (2002).
[44] E. Allahyarov, H. Löwen, A. A. Louis, and J.-P. Hansen, Europhys. Lett. **57**, 731 (2002).
[45] A. G. Moreira and R. R. Netz, Europhys. Lett. **57**, 911 (2002).
[46] P. Linse, J. Phys. Chem. **90**, 6821 (1986).